André Laschewsky, H. Ringsdorf, G. Schmidt

Polymerization of hydrocarbon and fluorocarbon amphiphiles in Langmuir-Blodgett multilayers

first published in:
Thin Solid Films. - 134 (1985), 1-3, p. 153 - 172
ISSN: 0040-6090
DOI: 10.1016/0040-6090(85)90127-0

Thin Solid Films, *134* (1985) 153–172

POLYMERIZATION OF HYDROCARBON AND FLUOROCARBON AMPHIPHILES IN LANGMUIR–BLODGETT MULTILAYERS*

A. LASCHEWSKY, H. RINGSDORF AND G. SCHMIDT
Institut für Organische Chemie und Institut für Physikalische Chemie der Universität Mainz (F.R.G.)
(Received April 25, 1985; accepted July 4, 1985)

Langmuir–Blodgett multilayers of polymerizable carboxylic acids with hydrocarbon or fluorocarbon chains were prepared. The multilayers were polymerized by UV light and the reactions were studied by UV/visible spectroscopy. The polyreactions strongly influence the multilayer structures which were investigated by X-ray small-angle scattering and scanning electron microscopy. The spreading behaviour of the monomers, the preparation of multilayers, their reactivities in multilayers and structural effects caused by the polyreactions are discussed with regard to the hydrophilic head groups, the polymerizable groups and the hydrophobic chains.

1. INTRODUCTION

Recently, Langmuir–Blodgett (LB) multilayers[1] have found an increasing interest for a wide range of potential applications[2,3], by virtue of their unique combination of properties such as a defined structure and a controllable, homogeneous thinness of a few nanometres. However, the poor stability of LB films against most solvents, mechanical stress and ageing imposes a serious drawback on any practical utilization. Therefore, attempts have been made to overcome these problems by polymerization of the amphiphiles within the layers[4–6]: the covalent linkage of the molecules stabilizes the multilayers. But, to date, few systematic studies of polymerizations in multilayers have been reported, and little is known about the influence of the polymer chain formed on the multilayer structure.

To investigate the influence of the polymerizable unit, the hydrophilic head group and the hydrophobic tail on the polymerization behaviour in multilayers, a variety of carboxylic acids containing the acrylic, the dienoyl, the diyne and the cinnamoyl moiety were synthesized (Table I). The amphiphiles were divided into five groups: unsaturated fatty acids (**1–3**), monoesters of dicarboxylic acids with long-chain hydrocarbon alcohols (**4–6**), monoesters of dicarboxylic acids with long-chain

* Paper presented at the Second International Conference on Langmuir–Blodgett Films, Schenectady, NY, U.S.A., July 1–4, 1985.

0040-6090/85/$3.30

fluorocarbon alcohols (**7–9**), cinnamoyl derivatives (**10, 11**), and bipolymerizable amphiphiles (**12–16**) which contain two different polymerizable moieties[7], as shown in Scheme 1 (where X denotes reactive group 1 and Z denotes reactive group 2). Except in compound **1**, the polymerizable groups are integral parts of the hydrophilic head group.

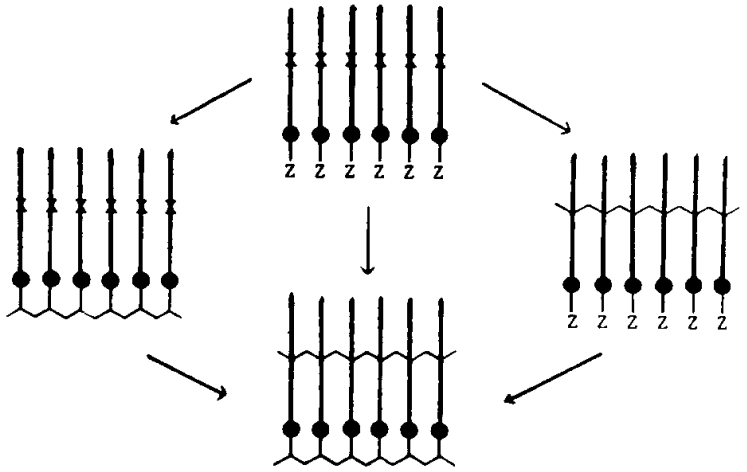

Scheme 1

The similar hydrocarbon and fluorocarbon monoesters, **4–6** and **7–9** respectively, allow comparative investigations of polymerizable fluorocarbon multilayers. The latter are of special interest because they offer new properties from multilayer systems controlled by the hydrophobic chain[8,9]; for example, fluorocarbons are chemically resistant and more hydrophobic than hydrocarbons. Hence, shorter hydrophobic tails can be used and thinner multilayers can be prepared. Furthermore, the permeability, miscibility, solubility and wetting properties of fluorocarbons differ markedly from these same properties in hydrocarbons[8].

2. MATERIALS AND METHODS

2.1. Materials

Compound **4** was supplied by Merck. Muconic acid was supplied by Aldrich, 4-hydroxycinnamic acid by Merck, octadecanol by Fluka and 1*H*,1*H*,11*H*-perfluoroundecanol by Kodak. The synthesis of the intermediates octadecanol[10] and heptacosa-10,12-diynol[6], and of the compounds **3**[11], **8**[12], **11**[13] and **15**[8] were each according to the synthesis of analogous compounds. The esters **5**, **12**, **14** and **16** were prepared from the acid chlorides and the alcohols. **7** was prepared by reaction of monomethyl fumarate with 1*H*,1*H*,11*H*-perfluoroundecanol in the melt at 150 °C. The syntheses of **1**[14], **2**[15], **6**[16], **9**[8], **10**[17] and **13**[18] are described elsewhere. All compounds were characterized by elemental analysis, ^{1}H–NMR, IR and field desorption mass spectroscopy. The melting points are given in Table I.

2.2. Monolayer experiments

Monolayer experiments were performed on a computer-controlled film balance[19]. The water was purified by a Milli-Q water purification system (Millipore

TABLE I

POLYMERIZABLE AMPHIPHILES FOR LB MULTILAYERS

Amphiphile	*Melting point*
Unsaturated fatty acids	
1 $CH_3(CH_2)_{12}-C{\equiv}C-C{\equiv}C-(CH_2)_8COOH$ / Cadmium salt	
2 $CH_3(CH_2)_{21}-C{\equiv}C-C{\equiv}C-COOH$	86
3 $CH_3(CH_2)_{16}-CH{=}CH-CH{=}CH-COOH$	85[a]
Monoesters of hydrocarbon alcohols	
4 $CH_3(CH_2)_{16}-CH_2-OOC-CH{=}CH-COOH$ trans	94
5 $CH_3(CH_2)_{16}-CH_2-OOC-CH{=}CH-CH{=}CH-COOH$ trans	104
6 $CH_3(CH_2)_{16}-CH_2-OOC-CH_2-C(=CH_2)-COOH$	86
Monoesters of fluorocarbon alcohols	
7 $H-(CF_2)_{10}-CH_2-OOC-CH{=}CH-COOH$ trans	142
8 $H-(CF_2)_{10}-CH_2-OOC-CH{=}CH-CH{=}CH-COOH$ trans	162
9 $CF_3-(CF_2)_9-CH_2-CH_2-OOC-CH_2-C(=CH_2)-COOH$	116
Cinnamoyl derivatives	
10 $CH_3(CH_2)_{16}-CH_2-O-C_6H_4-CH{=}CH-COOH$	148[b]
11 $(CH_3(CH_2)_{16}-CH_2-OOC)_2C{=}CH-C_6H_4-COOH$	89/96[c]
Bipolymerizable amphiphiles	
12 $CH_3(CH_2)_{13}-C{\equiv}C-C{\equiv}C-(CH_2)_8-CH_2-OOC-CH{=}CH-COOH$ trans	91
13 $CH_3(CH_2)_{13}-C{\equiv}C-C{\equiv}C-(CH_2)_8-CH_2-OOC-CH{=}CH-COOH$ cis	59
14 $CH_3(CH_2)_{13}-C{\equiv}C-C{\equiv}C-(CH_2)_3-CH_2-OOC-CH{=}CH-CH{=}CH-COOH$ trans	98
15 $CH_3(CH_2)_{13}-C{\equiv}C-C{\equiv}C-(CH_2)_8-CH_2-COC-CH_2-C(=CH_2)-COOH$	87
16 $CH_3(CH_2)_{12}-C{\equiv}C-C{\equiv}C-(CH_2)_3-COO-C_6H_4-CH{=}CH-COOH$	140[d]

[a] Polymerization above 85 °C.

[b] Liquid crystalline, k 121, s 148, i.

[c] Double melting.

[d] Liquid crystalline, k 91, s 127, n 140, decomposition.

Corporation), pH 5.5. The amphiphiles **1–3** and **11** were spread from hexane solutions, the amphiphiles **4–6** and **12–15** from hexane/ethanol mixtures (9:1 v/v), and the amphiphiles **7–10** and **16** from chloroform/methanol mixtures (9:1 v/v). The solvents were all Uvasol grade (Merck). The concentration of the solutions was about 0.2 mg ml^{-1}. The compression rates of the surface pressure–area diagrams were about 0.5 nm^2 $molecule^{-1}$ min^{-1}.

2.3. Multilayer preparation

The build up of multilayers was performed on a commercial film balance (Teflon-coated brass, Lauda). All amphiphiles were spread and deposited on pure aqueous subphases, except **1** which was spread on subphases containing 1 g $CdCl_2 \cdot H_2O$ l^{-1}. As supports, hydrophobized[20] quartz slides (Suprasil, Hereaus–Schott), polypropylene membranes (Celgard 2400, Celanese) and polyester foil (Hostaphan RE 3,0, Kalle) were used. The flexible polymer supports had to be backed by Teflon slides[22]. The area coated was 5 cm × 2.5 cm. After each dipping cycle, the supports were completely pulled out of the subphase and the samples were allowed to dry.

2.4. Polymerization of multilayers

The amphiphiles were polymerized in multilayers by UV light in air at room temperature. Two different UV lamps were used. Lamp A is a low-pressure mercury lamp with unfiltered UV light (Hamamatsu Corporation, model no. 937-002). Lamp B is a filtered low-pressure mercury lamp (Hereaus, Type 5340, 6 Watt) with 230 nm $< \lambda <$ 410 nm. In general, lamp B was used for polymerization. Lamp A was used only for monomers absorbing below 230 nm.

2.5. Characterization of multilayers

For UV/visible investigations, multilayers were built on quartz slides. The spectra were recorded with a Beckmann DU 6 spectrophotometer.

For small-angle X-ray scattering (SAXS) studies, multilayers were built on the smooth polyester foil. The experiments were performed with an X-ray powder diffractometer Siemens Type D 500 using the Cu Kα line (λ = 0.1541 nm). The layer spacings were calculated from the Bragg equation.

Scanning electron microscopy (SEM) investigations were performed with a Cambridge Mark II A. The samples were sputtered with gold.

3. RESULTS AND DISCUSSION

3.1. Spreading behaviour of the monomers

The spreading behaviour of the amphiphiles **1–16** is shown in Figs. 1–10. The surface pressure–area diagrams of all compounds show condensed phases at 20 °C. No phase transition up to 45 °C is found for **2, 3, 5, 7, 8, 10–12, 14** and **16**. Comparing the *hydrocarbon and fluorocarbon monoesters* **4–6** and **7–9**, the collapse areas of the hydrocarbons **4–6** are about 0.2 nm^2 $molecule^{-1}$, corresponding to a tight packing of the chains (Figs. 3–5). The fluorocarbons **7–9** show collapse areas of about 0.28 nm^2 $molecule^{-1}$ (Figs. 3, 4 and 6), because of the increased size of the CF_2 groups[8].

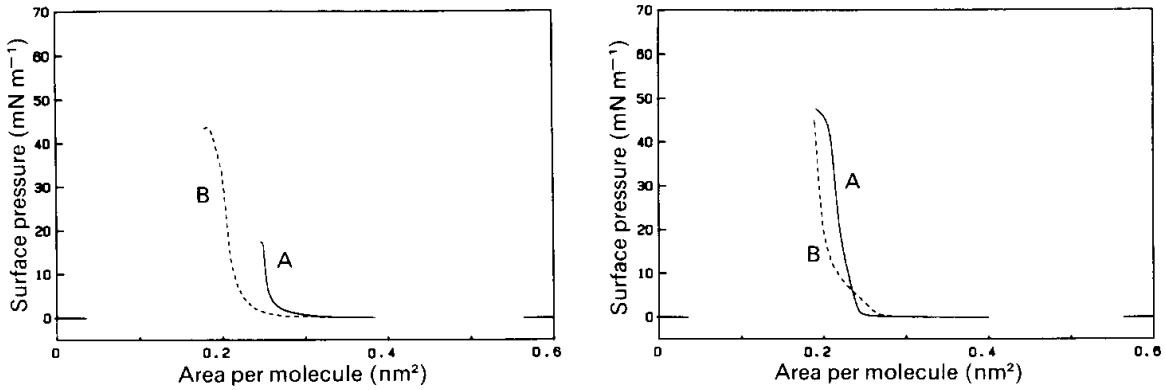

Fig. 1. Surface pressure–area diagrams for **1** at 20 °C: curve A, on water; curve B, on subphases containing $CdCl_2 \cdot H_2O$ (1 g l^{-1}).

Fig. 2. Surface pressure–area diagrams for the fatty acids **2** and **3** on water at 20 °C: curve A, **2**; curve B, **3**.

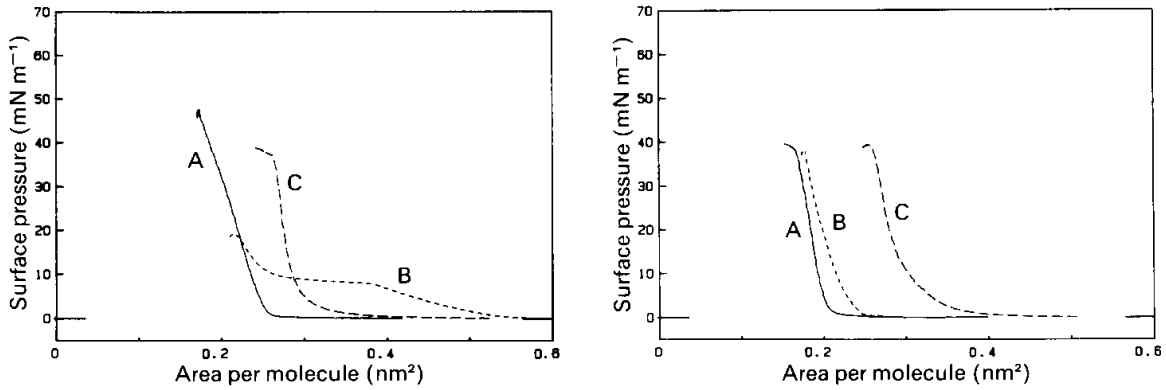

Fig. 3. Surface pressure–area diagrams for the fumarates **4** and **7** on water: curve A, **4** at 20 °C; curve B, **4** at 43 °C; curve C, **7** at 20 °C.

Fig. 4. Surface pressure–area diagrams for the muconates **5** and **8** on water: curve A, **5** at 20 °C; curve B, **5** at 45 °C; curve C, **8** at 20 °C.

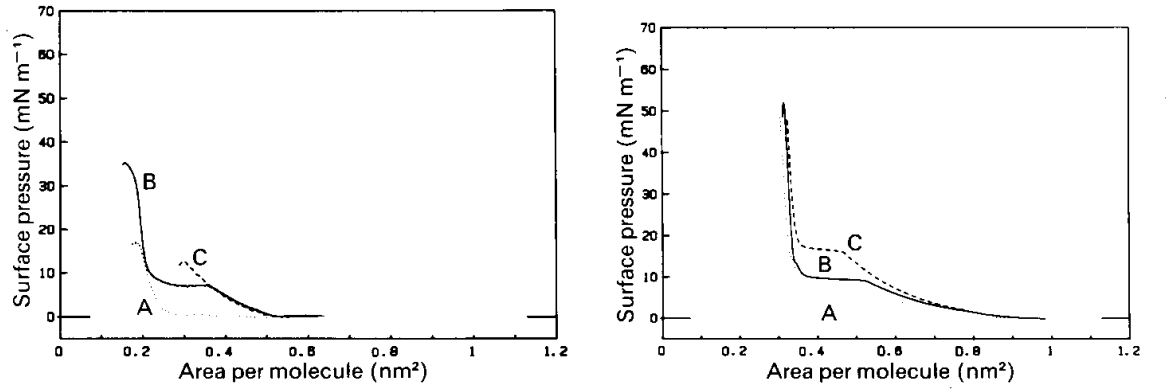

Fig. 5. Surface pressure–area diagrams for the itaconate **6** on water: curve A, at 10 °C; curve B, at 20 °C; curve C, at 40 °C.

Fig. 6. Surface pressure–area diagrams for the itaconate **9** on water: curve A, at 5 °C; curve B, at 20 °C; curve C, at 40 °C.

Hence, neither in the hydrocarbons nor in the fluorocarbons do the ester bonds prevent tight chain packing. The phase transitions of all fluorocarbons occur at much higher temperatures than those of their hydrocarbon analogues, in spite of the

much shorter chain lengths. This is caused by the stronger hydrophobic effect of fluorocarbons[8].

For the *cinnamoyl derivative* **10**, the minimal area occupied is about 0.22 nm^2 $molecule^{-1}$, corresponding to a tight packing of the aromatic cores (Fig. 7). Interactions of the aromatic cores probably cause the extreme rigidity of the monolayers of **10** and **11**.

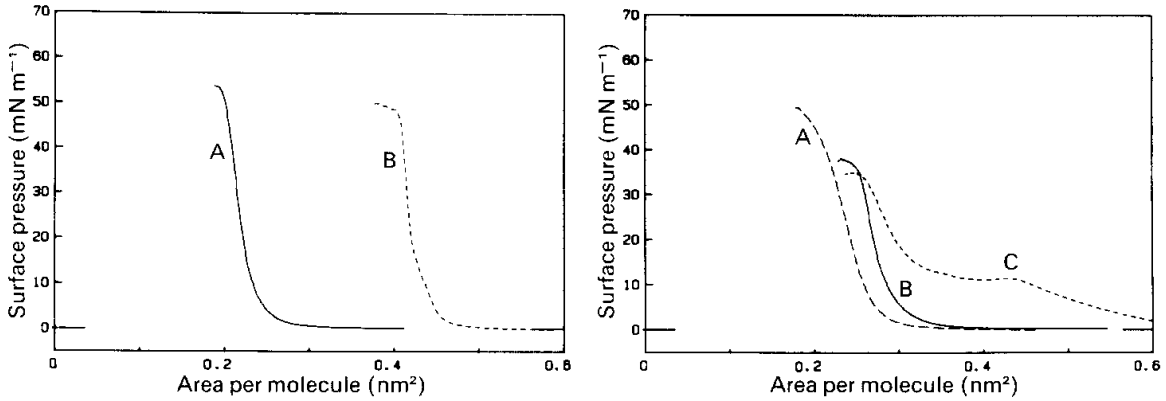

Fig. 7. Surface pressure–area diagrams for the cinnamoyl derivatives **10** and **11** on water at 20 °C: curve A, **10**; curve B, **11**.

Fig. 8. Surface pressure–area diagrams for **12** and **13** on water: curve A, **12** at 20 °C; curve B, **13** at 20 °C; curve C, **13** at 30 °C.

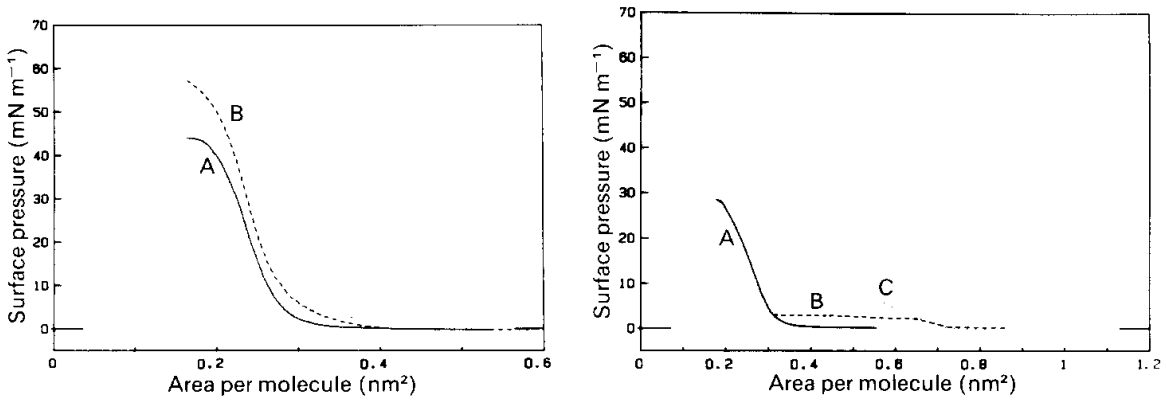

Fig. 9. Surface pressure–area diagrams for **14** and **16** on water at 20 °C: curve A, **14**; curve B, **16**.

Fig. 10. Surface pressure–area diagrams for **15** on water: curve A, at 20 °C; curve B, at 34 °C; curve C, at 45 °C.

The *diyne fatty acids* **1** and **2** and the *bipolymerizable amphiphiles* **12–16** exhibit collapse areas of about 0.25 nm^2 $molecule^{-1}$; the diyne moiety restricts the packing of the chains[21] (Figs. 1, 2 and 8–10).

Considering the *phase transitions*, the monoesters with identical chains, **4–6**, **7** and **8** and **12–15**, show decreasing transition temperatures T_G in the order muconate > fumarate > itaconate > maleate (Figs. 3–10). This order agrees with the order of the melting points, corresponding to the increasing difficulty of tight packing of the head groups, thus disturbing the packing of the chains and lowering T_G.

3.2. *Multilayer deposition*

Except for amphiphiles **1**[22] and **15**, all carboxylic acids investigated form condensed, stable monolayers on pure aqueous subphases at 20 °C. They can be deposited on hydrophobic supports without the use of salts of bivalent cations in the subphase. Thus, the use of cadmium salts can be avoided, of which the toxicity has limited many potential applications in the past. Possibly, the increased acidity of the α,β-unsaturated carboxylic acids eases the deposition process.

Table II lists the conditions applied for the preparation of the multilayers. As higher mobilities of the monolayers allow faster dipping speeds, the unsaturated fatty acids **1–3** can be deposited most rapidly. Because of the extreme low mobility of the cinnamoyl derivatives **10** and **11**, temperatures above 30 °C are required for the deposition process.

TABLE II
CONDITIONS APPLIED FOR MONOLAYER DEPOSITION

Amphiphile	*Temperature* (°C)	*Surface pressure* (mN m^{-1})	*Dipping speed* (cm min^{-1})		*Drying period* (min)	*Deposition type*
			Downwards	*Upwards*		
1	20	25	5	2	1	Y
2	20	20	5	2	3	Y
3	20	28	5	2	2	Y
4	20	30	3	2	2	Y
5	20	25	3	2	2	Y
6	20	22	3	2	1	Y
7	20	25	3	2	1	Y
8	20	20	3	2	1	Y
9	20	28	5	2	1	Y
10	32	32	3	0.5	1	Z
11	32	25	3	2	1	Y
12	20	20	3	2	2	Y
13	20	25	3	2	2	Y
14	20	20	3	2	2	Y
15	Monolayer not long-term stable					
16	20	25	3	2	2	Y

To achieve good coating qualities, all samples must be completely dry before transferring the next monolayer. Otherwise the last transferred monolayer is partially lost at the following dipping run, and the transfer ratio decreases with the number of layers deposited.

3.3. *Polymerization of monofunctional amphiphiles in multilayers*

The polymerizations in multilayers are easily performed by exposure of the monomeric multilayers to high-energy radiation, *e.g.* to UV light. Figures 11–22 and

Tables III and IV illustrate the polyreactions as followed by UV/visible spectroscopy.

It is known that diyne monomers polymerize under topochemical control in the solid state and in self-organized assemblies[23]. Because of the conjugated ene–ine backbone of the polymers, strongly coloured polymers are yielded, preferentially blue and red ones, depending on the polymer conformation[24].

Figure 11 shows the UV/visible spectra of **1** in dependence on the irradiation time with the filtered lamp B. After up to 20 min of irradiation, a blue polymer is formed with the maximum of the absorbance at 640 nm (polymer I). Further irradiation produces additional bands at shorter wavelengths. Absorbance maxima at 660 nm, 610 nm, 540 nm and 495 nm are observed. The spectrum does not change on irradiation for more than 240 min. A short treatment of the samples with warm (50 °C) methanol changes the colour irreversibly to red[25], and the polymer spectrum shows absorbance maxima at 540 nm and 495 nm only (polymer II). It should be noted that the polymerization behaviour and the absence of photobleaching is in contrast to previous studies of the polymerization of **1**[22] by irradiation with the unfiltered lamp A.

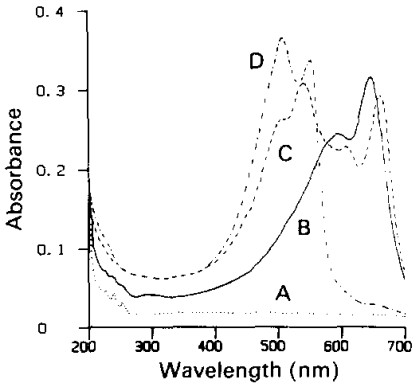

Fig. 11. UV/visible spectra of 40 layers of **1** as a function of irradiation time with filtered lamp B: curve A, 0 min; curve B, 20 min; curve C, 240 min; curve D, 240 min, additionally treated with warm methanol.

Compound **2**, with the diyne moiety in conjugation to the carboxylate, yields less intensely coloured polymers than **1**[26,27]. Only one polymer modification with a broad absorbance between 680 nm and 400 nm is found (Fig. 12). When the polymer is irradiated for longer than 20 min, its absorbance decreases slowly, probably as a result of photobleaching processes.

The irradiation of the *dienoic* acid **3** with the filtered lamp B is assumed to yield the 1,4-polymer (polymer I)[11,28]. The shoulder of the newly formed double bond at 190 nm can be seen clearly in Fig. 13. It can be reacted in a second step by irradiation with lamp A, to yield a cross-linked polymer, presumably by dimerization of the double bonds.

Similarly, the *muconates* **5** and **8** react in two steps. They seem to behave as two acrylic moieties, which can react independently. This is shown by the formation of a new absorption maximum at 218 nm on irradiation with the filtered lamp B (Figs. 14 and 15, polymers I). The new bands disappear on additional irradiation with lamp A (polymers II). Whether the reactions are polymerizations or dimerizations is

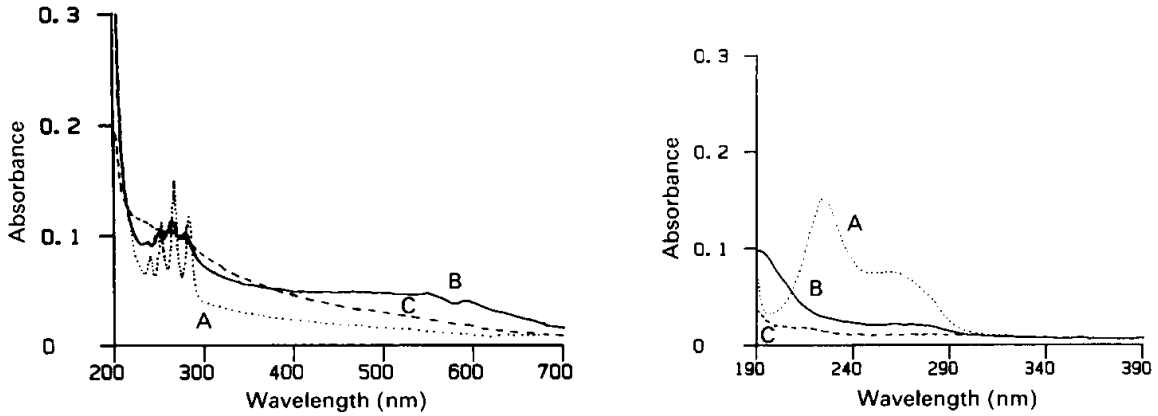

Fig. 12. UV/visible spectra of 40 layers of **2** as a function of irradiation time with filtered lamp B: curve A, 0 min; curve B, 12 min; curve C, 60 min.

Fig. 13. UV/visible spectra of 20 layers of **3** as a function of irradiation time with filtered lamp B: curve A, 0 min; curve B, 30 min; curve C, 30 min and also 90 min with unfiltered lamp A.

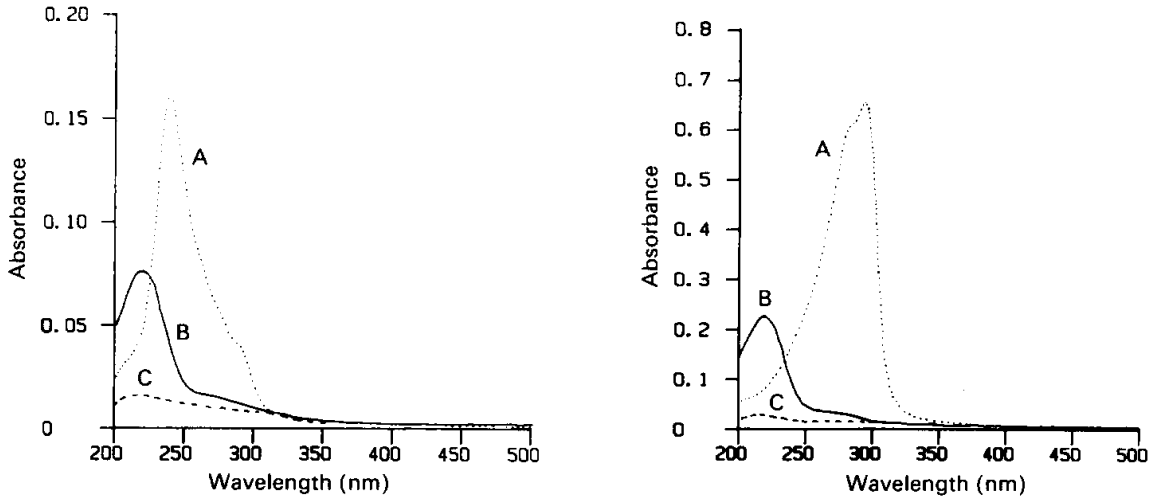

Fig. 14. UV/visible spectra of 20 layers of **5** as a function of irradiation time with filtered lamp B: curve A, 0 min; curve B, 30 min; curve C, 30 min and also 120 min with unfiltered lamp A.

Fig. 15. UV/visible spectra of 40 layers of **8** as a function of irradiation time with filtered lamp B: curve A, 0 min; curve B, 15 min; curve C, 30 min and also 90 min with unfiltered lamp A.

uncertain[7,28,29]. In any case, polymeric products are formed finally. It should be noted that the spectra of the hydrocarbon **5** and the fluorocarbon **8** differ strongly, although both have the same chromophore. Thus, the orientation and environment of the chromophores must be different.

The *fumarates* **4** and **7** and the *itaconates* **6** and **9** exhibit a single absorption band which decreases on UV irradiation with lamp A (Table IV, Figs. 19 and 21). The formation of polymers of the fumarate **4** was shown by NMR spectroscopy. Interestingly, in some cases the maximum of the monomer absorbance changes continuously with the irradiation time. This will be discussed with the SAXS data below.

The UV/visible spectra of the cinnamoyl derivatives **10** and **11** are presented in Figs. 16 and 17. For both, remarkably low conversions of the dimerization reactions[17] are found (Fig. 22). Irradiation beyond 180 min leads to neither further polyreaction nor notable photobleaching.

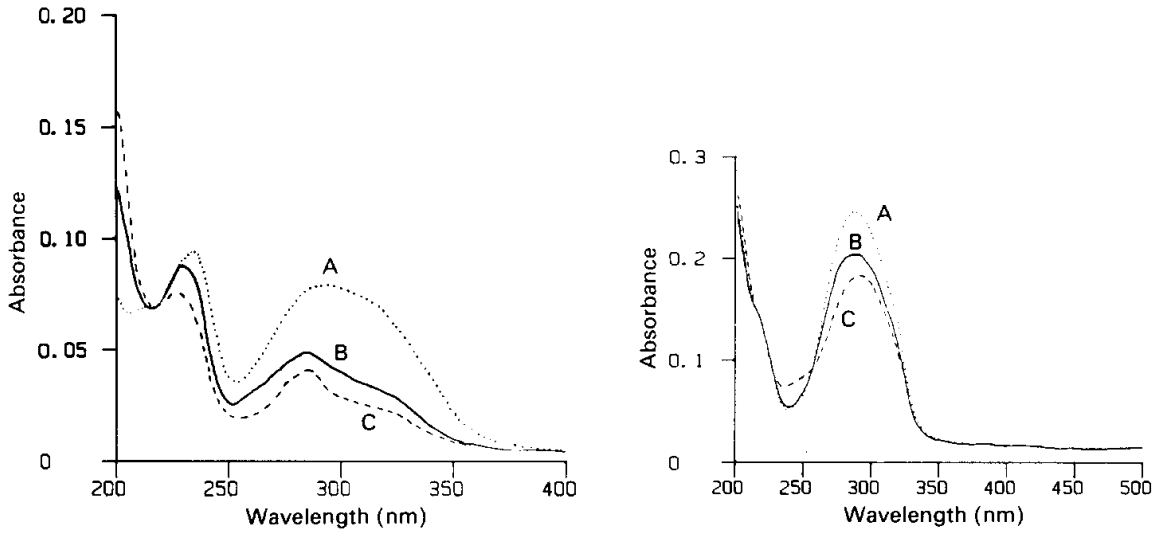

Fig. 16. UV/visible spectra of 20 layers of **10** as a function of irradiation time with filtered lamp B: curve A, 0 min; curve B, 5 min; curve C, 120 min.

Fig. 17. UV/visible spectra of 36 layers of **11** as a function of irradiation time with filtered lamp B: curve A, 0 min; curve B, 10 min; curve C, 180 min.

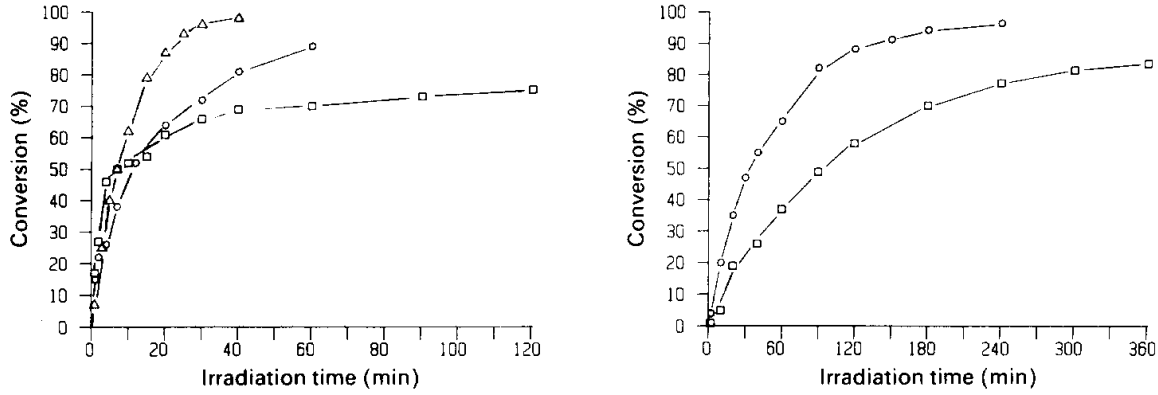

Fig. 18. Monomer conversions of the fatty acids **1–3** as a function of irradiation time with filtered lamp B: □, **1**; ○, **2**; △, **3**.

Fig. 19. Monomer conversions of the fumarates **4** and **7** as a function of irradiation time with unfiltered lamp A: □, **4**; ○, **7**.

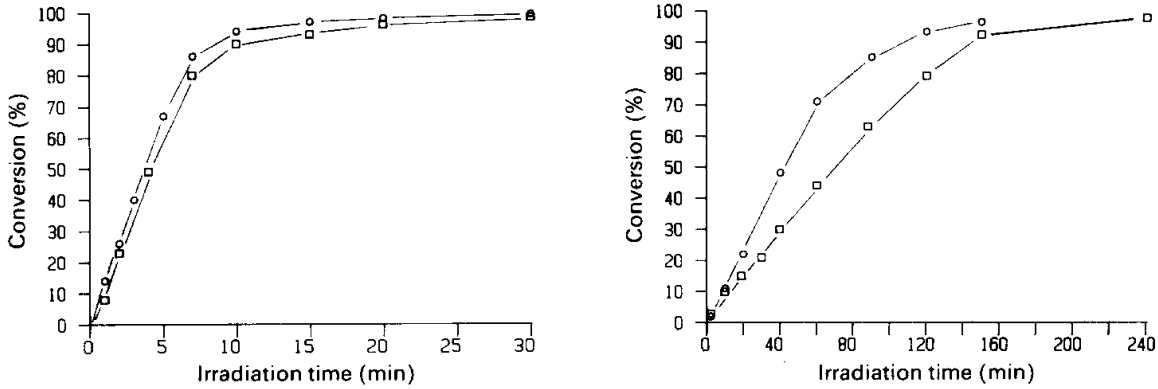

Fig. 20. Monomer conversions of the muconates **5** and **8** as a function of irradiation time with filtered lamp B: □, **5**; ○, **8**.

Fig. 21. Monomer conversions of the itaconates **6** and **9** as a function of irradiation time with unfiltered lamp A: □, **6**; ○, **9**.

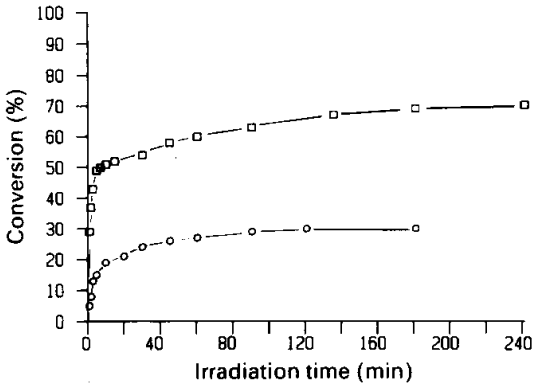

Fig. 22. Monomer conversions of the cinnamoyl derivatives **10** and **11** as a function of irradiation time with filtered lamp B: □, **10**; ○, **11**.

TABLE III

UV IRRADIATION[a] TIMES FOR POLYMERIC MULTILAYERS OF THE MULTIFUNCTIONAL AMPHIPHILES **1–11**

Amphiphile	*Irradiation time* (min)	
	Polymer I	*Polymer II*
1	20(B)	240(B)[b]
2	20(B)	—
3	30(B)	30(B)+90(A)
4	360(A)	—
5	30(B)	30(B)+120(A)
6	180(A)	—
7	180(A)	—
8	20(B)	30(B)+90(A)
9	150(A)	—
10	120(B)	—
11	180(B)	—

[a] (A), irradiated with the unfiltered lamp A; (B), irradiated with the filtered lamp B.
[b] Additionally treated with warm methanol.

TABLE IV

POLYMERIZATION BEHAVIOUR OF THE MONOFUNCTIONAL AMPHIPHILES **1–11**

Amphiphile	*Absorption bands studied* (nm)	*Conversion achieved* (%)	*Shift of monomer absorption maximum*
1	210–275	80±15	
2	230–300	90±10	
3	200–310	100	
4	214	85±10	214 → 206
5	200–350	100	240 → 245
6	210	100	210 → 205
7	210	98±5	No shift observed
8	200–350	100	292 → 286
9	209	100	No shift observed
10	250–400	70±5	
11	240–350	30±5	

3.4. Polymerization rates and monomer conversions of the monofunctional amphiphiles

The efficiency of the polyreactions depends on factors such as the reaction rate and the maximal conversion of the monomers. Both factors were studied for the polymerizable amphiphiles **1**–**11**.

UV/visible spectroscopy was chosen to determine the rate and the degree of the monomer conversions, by recording the decrease of the monomer absorbances. In addition to the polymerizations and dimerizations, photobleaching processes have to be considered as a possible source of monomer absorbance decrease. However, photobleaching processes seem to be negligible, because in cases of incomplete conversion the residual monomer absorbance remains almost constant even after hours of additional irradiation (Figs. 18 and 22).

Figures 18–22 show the time conversion curves of **1**–**11** as measured by the decrease of the monomer absorbance. Complete conversion is always observed, if the polymerization is not topochemically controlled (Table IV, compounds **3**, **5**, **6**, **8** and **9**). Under topochemical control, for each compound a characteristic value of maximal conversion is approached asymptotically (Table IV, compounds **1**, **2**, **4**, **7**, **10** and **11**). This means, either only part of the monomers is arranged well enough for the topochemical reaction, or the reaction changes the arrangement of the residual monomers until the reaction cannot proceed any more.

A comparison of the hydrocarbon monoesters **4**–**6** and their fluorocarbon analogues **7**–**9** illustrates the influence of the hydrophobic chains on the polyreaction (Figs. 19–21). The topochemical polymerization of the fluorocarbon fumarate **7** leads to much higher conversion than that of the hydrocarbon fumarate **4**. Whereas the reactivities of both the muconates **5** and **8** are comparable, the fluorocarbons **7** and **9** react much faster than their hydrocarbon analogues **4** and **6**. This reflects the strong influence of the hydrophobic chains on the polymerization, even if the polymerizable group is located in the hydrophilic head. The influence is not restricted to topochemically controlled reactions, as shown by the reactions of the itaconates **6** and **9**. This influence will be discussed with the SAXS data below.

3.5. Polymerization of bifunctional amphiphiles in multilayers

The bipolymerizable amphiphiles **12**–**14** and **16** (UV irradiation times shown in Table V) behave individually. In the cases of **12**–**14** and **16**, the blue or red colour of

TABLE V

UV IRRADIATION[a] TIMES FOR POLYMERIC MULTILAYERS OF THE BIFUNCTIONAL AMPHIPHILES **12**–**16**

Amphiphile	*Irradiation time* (min)	
	Polymer I	*Polymer II*
12	30(A)	120(A)
13	20(B)	120(B) + 150(A)
14	40(B)	90(B) + 90(A)
15	—	
16	5(B)	120(B)

[a] (A), irradiated with the unfiltered lamp A; (B), irradiated with the filtered lamp B.

the polymers formed indicates the successful topochemical polymerizations of the diyne units, whereas the diyne unit in compound **15** could not be polymerized by UV light.

Irradiation of the *fumarate* **12** with the filtered lamp B does not yield polymer, although the UV light is in the absorption region of the diyne moiety. Only on irradiation with the unfiltered lamp A does the fumarate absorbance at 210 nm decrease—and the diyne polymerizes simultaneously to yield weakly red coloured polymers (Fig. 23, polymer I). After 40 min of irradiation the polymerization of the fumarate still proceeds, whereas the absorption of the polymer decreases, which is attributed to photobleaching processes. After more than 120 min of irradiation, the residual absorbance of the fumarate remains constant (polymer II).

In contrast to the fumarate **12**, the *maleate* **13** can be polymerized in two steps (Fig. 24). Irradiation with the filtered lamp B ($\lambda > 230$ nm) yields the strongly blue coloured polydiacetylene, with maximal absorbance at 640 nm. The absorbance of the maleate at 200 nm does not change (polymer I). Subsequent irradiation with lamp A decreases the maleate absorption band and shifts the polymer absorption towards 545 nm and 500 nm, thus changing the colour of the polymer from blue via violet to red (polymer II). After more than 30 min of irradiation with lamp A, again photobleaching of the diyne polymer is found.

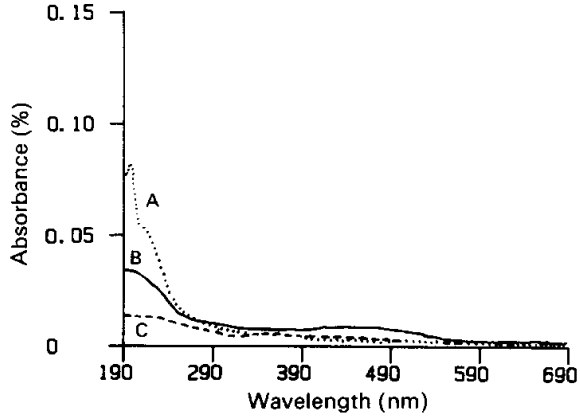

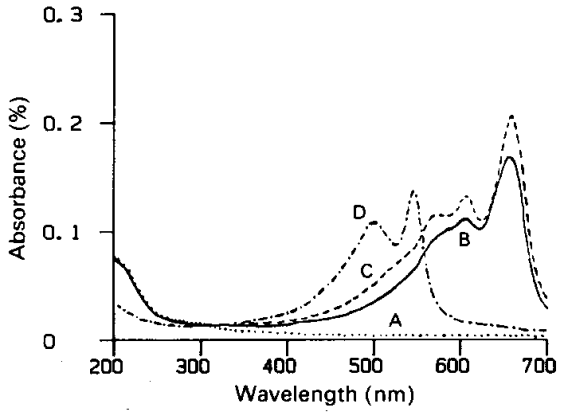

Fig. 23. UV/visible spectra of 20 layers of **12** as a function of irradiation time with unfiltered lamp A: curve A, 0 min; curve B, 30 min; curve C, 120 min.

Fig. 24. UV/visible spectra of 20 layers of **13** as a function of irradiation time with filtered lamp B: curve A, 0 min; curve B, 20 min; curve C, 120 min; curve D, 120 min and also 150 min with unfiltered lamp A.

Irradiation of the *muconate* **14** with lamp B yields red coloured polymer, the muconate and the diyne moiety reacting simultaneously (polymer I, Fig. 25). Like the muconates **5** and **8**, **14** shows the formation of a new band at 220 nm on irradiation with the unfiltered lamp B. This band decreases by irradiation with lamp A (polymer II). Prolonged exposure to UV light causes the usual photobleaching of the polymer absorption. The diyne and the *cinnamoyl* group of **16** react simultaneously to yield a blue polymer after 5 min of irradiation with lamp B (polymer I) with the absorbance maximum at 640 nm (Fig. 26). The polymer absorption is shifted to shorter wavelengths by further irradiation yielding after 2 h the red polymer (polymer II). Again, prolonged irradiation causes photobleaching of the polymer colour.

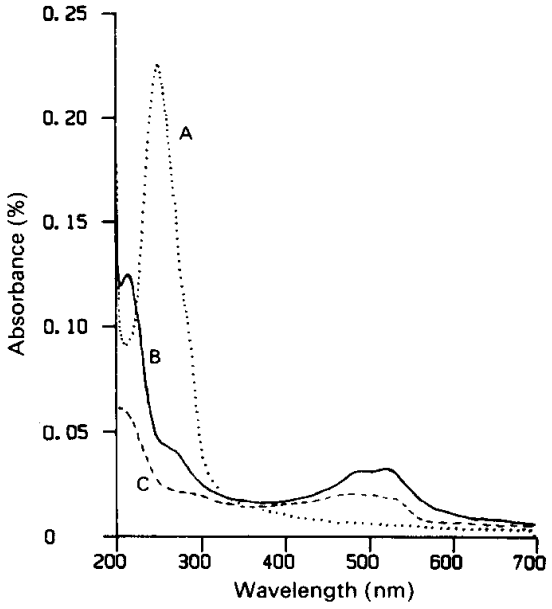

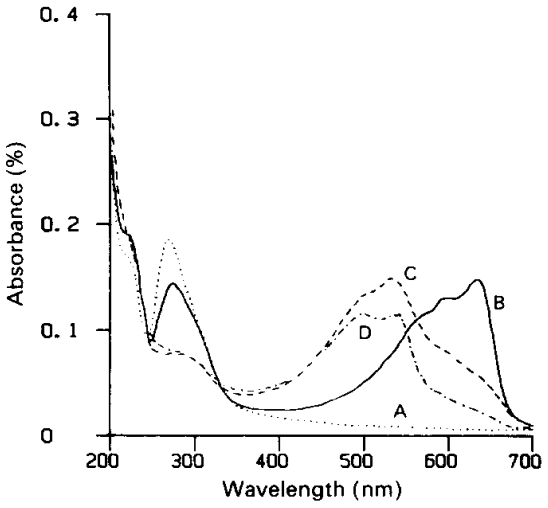

Fig. 25. UV/visible spectra of 20 layers of **14** as a function of irradiation time with filtered lamp B: curve A, 0 min; curve B, 40 min; curve C, 90 min and also 90 min with unfiltered lamp A.

Fig. 26. UV/visible spectra of 40 layers of **16** as a function of irradiation time with filtered lamp B: curve A, 0 min; curve B, 5 min; curve C, 80 min; curve D, 120 min.

The individual behaviour of the diyne unit in the bipolymerizable amphiphiles is probably due to the topochemical control of the diyne polymerization. Small differences in the arrangement of the monomers result in strongly different polymerization behaviour[23]. Accordingly, unfavourable arrangement has to be blamed for the missing photoreactivity of **15**.

3.6. Small-angle X-ray scattering (SAXS) investigations

The multiple sandwich bilayer structure of multilayers represents a perfect layer lattice. This results in X-ray diagrams with narrow scattering reflections of several orders. Thus, the layer spacings can be determined within an error of $< 1\%$. Because of the tight packing of the chains, the amphiphiles take their maximally stretched conformation in the layers. Hence, the spacings determined by SAXS can be compared with the calculated ones[27,30].

The spacings of the multilayers of **1**–**14** and **16** are listed in Table VI. For all amphiphiles investigated, the spacings determined are less than the calculated ones. This is attributed to the tilt of the amphiphiles in the layers[27,30]. As reported for some multilayer systems, the spacings change during the polyreaction[26,27,30,31]. This effect is not restricted to topochemically controlled polyreactions as are those of **1**, **2**, **4**, **7**, **10** and **11**, but is a general feature of all the amphiphiles investigated. The spacings change continuously during the polymerization towards a final value; but there is no linear correlation of the conversion achieved, as determined by UV/visible spectroscopy. The range of the relative changes extends from -2% to $+29\%$ (Table VI).

The different polymer modifications of **1** and the different polymers of **3**, **5**, **8**, **12**–**14** and **16**, as observed by UV/visible spectroscopy (Figs. 13–15 and 23–26), can be clearly distinguished by SAXS too. If two subsequent polymers of a compound

TABLE VI

SPACINGS OF MONOMERIC AND POLYMERIC MULTILAYERS OF AMPHIPHILES **1–15** DETERMINED BY SAXS, 30 LAYERS DEPOSITED

Amphiphile	*Spacing of a sandwich bilayer* (nm)			
	Monomer	*Polymer I*	*Polymer II*	*Calculated*
1	5.68	5.77	6.15	7.1
2	5.05	5.32	—	7.2
3	5.06	5.32	—	6.3
4	4.41	5.68	—	6.6
5	5.26	5.42	5.48	7.1
6	4.44	4.67	—	6.3
7	3.86	3.82	—	4.8
8	4.08	4.25	4.12	5.3
9	3.90	3.87	—	5.1
10	5.66	5.59	—	7.0
11	5.98	6.13	—	7.3
12	5.92	6.15	[a]	8.7
13	5.83	5.92	6.65[b]	8.7
14	6.20	6.38	[a]	9.2
15	6.12	6.22	6.54	8.7

[a] No scattering reflection observed.

[b] Only the broadened first-order scattering reflection observed.

exist, the changes of the spacings can be opposite for each step, as **3** and **8** exemplify (Table VI).

In addition to the first-order reflections of the layers, reflections of higher orders are observed, *e.g.* up to twelve for **1** (30 layers deposited). In general, the odd-order reflections are relatively more intense than the even ones. On polymerization, the number of reflections of higher orders decreases[26,27].

However, for all the *monofunctional amphiphiles* **1–11**, *i.e.* for all the types of polyreactions investigated, the linewidth of the first-order reflection is essentially the same for monomeric and polymeric multilayers.

A comparison of the hydrocarbon monoesters **4–6** and their fluorocarbon analogues **7–9** is instructive. The data of Table VI show that both the tilt of the molecules and the change of the layer spacings depend on both the head group and the hydrophobic tail. The tilt angles of compounds with identical chains but different head groups, such as **4–6** or **7** and **8**, differ strongly. The same holds true for compounds with identical head groups but different hydrophobic chains such as **4** and **7**, **5** and **8** or **6** and **9**.

Remarkably, in the case of amphiphiles with identical reactive moieties, the polymer chain formed does not approximate the different orientations of the amphiphiles, which might have been expected; *i.e.* the structure of the polymeric multilayers is determined by the polymeric backbone and the head group and the

hydrophobic chain together. None of the structural elements on its own controls the polymeric multilayer structure formed.

Combining the data of Tables IV and VI, it can be seen that the amphiphiles with marked changes of layer spacings, such as **4–6** and **8**, show shifts of the monomer absorbance maxima during the polyreaction. In contrast, no shift of the monomer absorbance maxima is observed for **7** and **9** which both exhibit only slightly changed layer spacings. Obviously, the shift of the absorbance maxima is due to the altered environment of the chromophores somehow related to the altered orientation of the hydrophobic chains. The much smaller change of the layer spacings of **7** and **9** during the polymerization, compared to their analogues **4** and **6**, correspond to their much faster polyreactions (Figs. 19 and 21). In contrast, the analogues **5** and **8** show equal changes of layer spacings and equal polymerization reactivities (Fig. 20). Hence, the rate of polymerization seems to depend on the extent of the structural change of the multilayer occurring during the reaction.

The different polymers formed of the *bipolymerizable amphiphiles* **12–14** and **16** can be distinguished by SAXS clearly. **16** behaves similarly to the diynoic acid **1**. The blue polymer I is characterized by a slightly increased spacing of the layers of about 1.5%, whereas the red polymer II shows a spacing increased by about 8% compared to the monomer.

The results of the SAXS investigations obtained from **12–14** show an important new feature. In contrast to all monofunctional polymerizable amphiphiles **1–11** and to **16**, the polymers I still show sharp SAXS reflections, but the polymers II no longer do. In the case of **13**, the first-order reflection is strongly broadened. For the polymers II of **12** and **14** no more SAXS reflections are found (Table VI). Because the polymers of **4**, **6**, **7** and **9** with high radiation doses (Tables III and V) still show unaffected, sharp reflections, the explanation of the lost reflections of **12** and **14** is rather more a multiple polymerization than an irradiation effect. The two polymeric backbones formed seem to interfere, and thus cause severe distortions of the multilayer structure.

Accordingly, the broadened, but still existent first-order reflection of the polymer of **13** suggests that the reaction of the maleate yields oligomers only, so keeping the distortion of the multilayers moderate. This agrees well with the fact that the simultaneous polymerization of the diyne group and the dimerization of the cinnamoyl group of **16** do not damage the layer structure; *i.e.* basically cross-linking of polymeric chains is possible in multilayers without harm.

Based on these considerations, the second reaction step of the butadiene **3** leading to its polymer II, and at least one step of the reactions of the muconates **5** and **8** should lead to dimers or low oligomers, because the respective polymeric multilayers show unaffected sharp SAXS reflections.

3.7. Investigations by scanning electron microscopy (SEM)

The SAXS investigations of the multilayers demonstrate the change of the layer spacings by the polyreactions, which can be as extreme as 30% difference between monomeric and polymeric layers (Table VI). The question now arises: how is the stability and the perfection of the multilayers affected by the structural change?

Because it is difficult to measure these properties absolutely, a relative method

was chosen. The ability of multilayers to bridge pores of the support material was used to judge the relative stability. The pores act as probes for the quality of the multilayers. Large defects in the layers are easily detected by SEM[22]. A porous polypropylene membrane (Celgard 2400) was chosen as support, of which the pores, about 0.2 μm in diameter, are known to be bridged by good-quality multilayers[22,32].

The results of the SEM investigations are presented in Table VII. Accordingly, several groups of amphiphiles can be distinguished. **5**, **10** and **11** show both perfect monomeric and polymeric/dimeric multilayers. In the cases of **1**, **4**, **12–14** and **16**, the monomeric layers look perfect; however, defects can be found in the polymerized layers[32,33] (Fig. 27), depending on the number of layers deposited.

The last group is represented by **6–9** of which the multilayers cannot bridge pores in any of the cases investigated. The existence of defects in the multilayers above the pores can be caused by the inability of the amphiphiles to bridge large pores. In the cases of **6** and **9**, the itaconate head group might be responsible because of its unfavourable geometry. This would be in agreement with the unstable monolayers of the itaconate **15**. It is striking that all the fluorocarbon amphiphiles cannot bridge the pores of the support, whereas the hydrocarbon analogues **4** and **5** do. The reason might be the reduced interaction between the fluorocarbon amphiphiles in the layers. The hydrophobic chains are very short (C_{12} only), and

TABLE VII

COATING PROPERTIES OF MONOMERIC AND POLYMERIC MULTILAYERS OF AMPHIPHILES **1–14** AND **16** ON CELGARD 2400 MEMBRANES STUDIED BY SEM[a]

Amphiphile	*Number of layers*								
	Monomer			*Polymer I*			*Polymer II*		
	2	*4*	*6*	*2*	*4*	*6*	*2*	*4*	*6*
1	+	+	+	+	+	+	○	+	+
2			+			+			+
3			+			+			+
4	+		+	○		○			
5	+		+	+		+	+		+
6	○		○	○		○			
7	○		○	○		○			
8	○		○	○		○			
9	○		○	○		○			
10	+		+	+		+			
11	+		+	+		+			
12			+			+			○
13			+			+			○
14	+		+	+		+	○		○
16	+	+	+	+	+	+	○	+	+

[a] +, all pores of the support coated; ○, pores of the support visible.

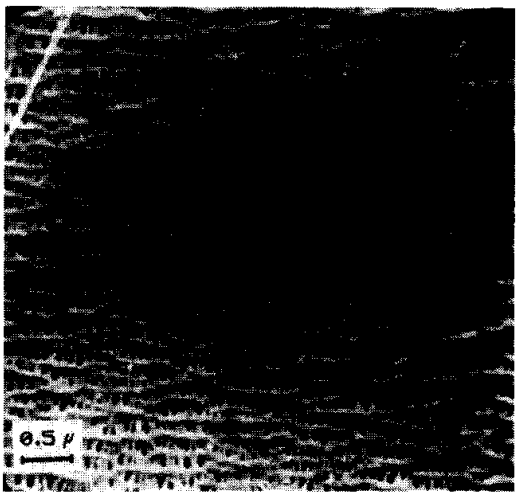

(a)

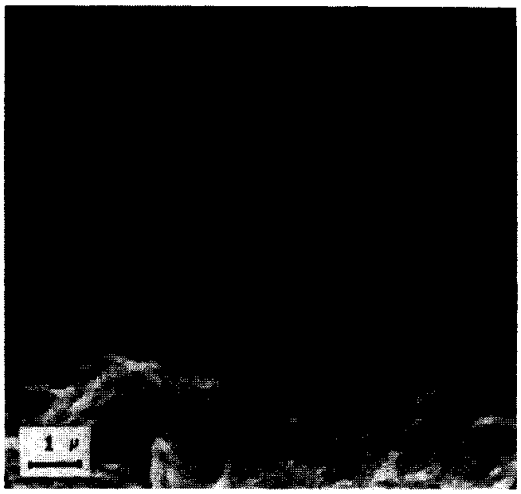

(b)

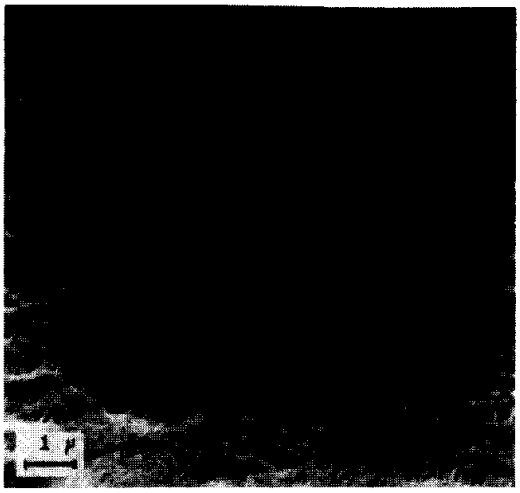

(c)

Fig. 27. Scanning electron micrographs of bilayers of **1** on porous polypropylene membranes (Celgard 2400): (a) uncoated support; (b) coated with polymer I (blue form); (c) coated with polymer II (red form).

interactions between fluorocarbons are known to be few, as the low melting enthalpies indicate[8]. Thus, the size of pores which can be bridged is decreased.

In the cases of **1**, **4**, **12–14** and **16**, defects in the layers are found only after polymerization of the layers. Being aware that the layer spaces might depend on the number of layers deposited in some cases,[30] we attempted to correlate the changes of the layer spacings determined by SAXS (Table VI) and the presence or absence of defects (Table VII), as done in Fig. 28. The plot shows that the presence of defects is a function of the relative change of the layer spacing and of the number of layers deposited. Small changes of the layer spacings do not cause defects. However, if the relative changes exceed a critical value, defects are formed. As the thicker multilayers show enhanced stability, the critical value for bilayers is about 5%, for six layers deposited it is about 10%, above which defects are found. Concerning the bipolymerizable amphiphiles **12–14**, all polymeric multilayers show defects in agreement with the discussion of the SAXS data.

It has to be kept in mind that the SEM investigations are still a crude method to judge the stability and the quality of multilayers. Only defects bigger than the

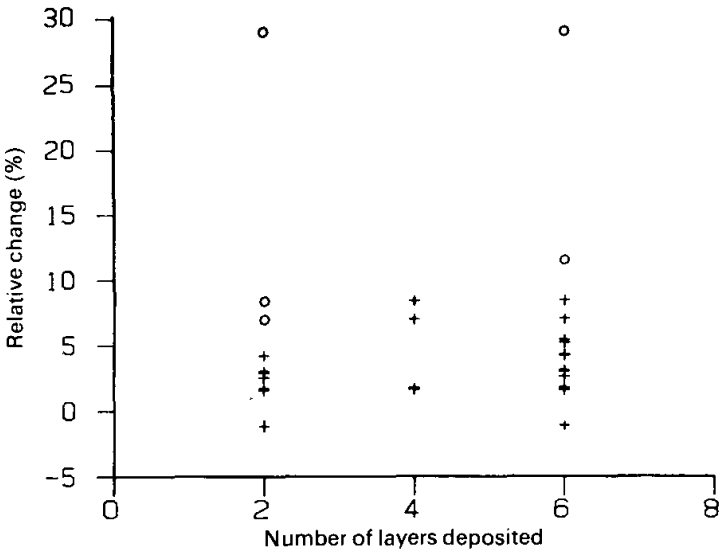

Fig. 28. Formation of defects in multilayers built up on Celgard 2400 by polyreactions, as observed by SEM. Dependence on the number of layers deposited and on the relative change of the layer spacings is shown. +, all pores of support coated after the polyreaction; ○, pores visible after the polyreaction. (Data taken from Tables VI and VII.)

resolution of the microscope (about 20 000× magnification) can be seen. Nothing is known about smaller defects. But the crucial point of the SEM findings is that defects in the layers can be caused by the polymerization. This means that the enhanced stability of polymeric multilayers is bound to a reduced quality. To keep the multilayer quality high, amphiphiles must be used, such as **3** or **5**, which undergo only minor structural changes of the multilayers by the polyreaction. Alternatively, spacer groups can be incorporated between the reactive group and the main amphiphilic part of the molecules, which minimize distortions of the layers by the polyreactions[33]. An additional approach would be multilayers built from pre-polymerized amphiphiles[33,34].

4. CONCLUSIONS

Multilayers can be prepared from a variety of polymerizable amphiphiles, including some with fluorocarbon chains. The multilayers were polymerized by UV light. Complete conversion of the monomers was achieved, except under topochemical polymerization control. For all amphiphiles investigated, the polymerization of the multilayers is bound to a change of the layer spacings. If different polymerizable groups are reacted in the amphiphiles, the interference of the different polymer backbones damages the multilayer structure. However, to enhance the stability of the layers, cross-linking via dimerization processes is possible without harm. The change of the layer spacings can cause the formation of defects in the multilayers. Comparing hydrocarbon and fluorocarbon analogues, the fluorocarbons are found to build multilayers more easily, in spite of their much shorter hydrophobic chains. The fluorocarbon multilayers can be easily polymerized with only slight changes of the layer spacings. Because of the reduced interactions of the short fluorocarbon chains, porous supports should be avoided for the deposition of fluorocarbon monolayers. However, the ease of the deposition, the fast polymerizations and the

thin multilayers obtained render the fluorocarbon amphiphiles valuable for multilayer applications.

REFERENCES

1 K. B. Blodgett and I. Langmuir, *Phys. Rev., 51* (1937) 964.
2 *Thin Solid Films, 68* (1980).
3 *Thin Solid Films, 99* (1983).
4 A. Cemel, T. Fort, Jr., and J. B. Lando, *J. Polym. Sci., Part A, 10* (1972) 2061.
5 R. Ackermann, D. Naegele and H. Ringsdorf, *Makromol. Chem., 175* (1974) 699.
6 B. Tieke, H. J. Graf, G. Wegner, D. Naegele, H. Ringsdorf, A. Banerjie, D. Day and J. B. Lando, *Colloid Polym. Sci., 255* (1977) 521.
7 A. Barraud, C. Rosilio and A. Ruaudel-Teixier, *Polym. Prepr., Am. Chem. Soc. Div. Polym. Chem., 19* (1978) 179.
8 R. Elbert, T. Folda and H. Ringsdorf, *J. Am. Chem. Soc., 106* (1984) 7687.
9 T. Kunitake, Y. Okahata and S. Yasunami, *J. Am. Chem. Soc., 104* (1982) 5547.
10 G. Piancatelli, A. Scettri and M. d'Auria, *Synthesis*, (1982) 245.
11 H. Ringsdorf and H. Schupp, *J. Macromol. Sci., Chem., 15* (5) (1981) 1015.
12 B. Neises and W. Steglich, *Angew. Chem., 90* (1978) 556.
13 G. Jones, *Org. React., 15* (1967) 204.
14 B. Hupfer, H. Ringsdorf and H. Schupp, *Chem. Phys. Lipids, 33* (1983) 355.
15 (a) M. Haubs and H. Ringsdorf, to be published.
(b) See ref. 25.
16 (a) R. Keller, *Master Thesis*, Mainz, 1982.
(b) K. Nyiatrai, N. L. Nguyen, F. Cser, E. Takacs and G. Hardy, *Acta Chim. Sci. Hung., 96* (1978) 223.
17 (a) H. Koch, A. Laschewsky, H. Ringsdorf and K. Teng, *Makromol. Chem.*, in the press.
(b) J. W. Cray and P. Jones, *J. Chem. Soc.*, (1954) 223.
(c) V. Enkelmann, B. Tieke, H. Kapp, G. Lieser and G. Wegner, *Ber. Bunsenges. Phys. Chem., 82* (1978) 875.
18 (a) H. Bader, Dissertation, Mainz, 1985.
(b) H. Bader and H. Ringsdorf, *Faraday Discuss. Chem. Soc., 81* (1986) in the press.
19 O. Albrecht, *Thin Solid Films, 99* (1983) 227.
20 H. Bücher, O. von Elsner, D. Möbius, P. Tillmann and J. Wiegand, *Z. Phys. Chem., NF, 65* (1969) 152.
21 B. Hupfer and H. Ringsdorf, *Chem. Phys. Lipids, 33* (1983) 263.
22 O. Albrecht, A. Laschewsky and H. Ringsdorf, *Macromolecules, 17* (1984) 937.
23 V. Enkelmann, G. Wenz, M. A. Müller, M. Schmidt and G. Wegner, *Mol. Cryst. Liq. Cryst., 105* (1984) 11.
24 G. N. Patel and N. L. Yang, *J. Chem. Educ., 60* (1983) 181.
25 B. Tieke, G. Lieser and G. Wegner, *J. Polym. Sci. Polym. Chem. Educ., 17* (1979) 1631.
26 B. Tieke and G. Lieser, *J. Colloid Interface Sci., 88* (1982) 471.
27 B. Tieke, G. Lieser and K. Weiss, *Thin Solid Films, 99* (1983) 95.
28 B. Tieke, *J. Polym. Sci. Polym. Chem. Educ., 22* (1984) 391.
29 M. Lahav and G. M. J. Schmidt, *J. Chem. Soc. B*, (1967) 312.
30 D. Naegele, J. B. Lando and H. Ringsdorf, *Macromolecules, 10* (1977) 1339.
31 A. Banerjie and J. B. Lando, *Thin Solid Films, 68* (1980) 67.
32 O. Albrecht, A. Laschewsky and H. Ringsdorf, *J. Membrane Sci., 22* (1985) 187.
33 R. Elbert, A. Laschewsky and H. Ringsdorf, *J. Am. Chem. Soc., 107* (1985) 4134.
34 R. H. Tredgold and C. Winter, *Thin Solid Films, 99* (1983) 81.